Front. Mech. Eng. 2017, 12(4): 459–476
DOI 10.1007/s11465-017-0462-x

REVIEW ARTICLE

Chuang YUE, Jing LI, Liwei LIN

Fabrication of Si-based three-dimensional microbatteries: A review

Abstract High-performance, Si-based three-dimensional (3D) microbattery systems for powering micro/nano-electromechanical systems and lab-on-chip smart electronic devices have attracted increasing research attention. These systems are characterized by compatible fabrication and integratibility resulting from the silicon-based technologies used in their production. The use of support substrates, electrodes or current collectors, electrolytes, and even batteries used in 3D layouts has become increasingly important in fabricating microbatteries with high energy, high power density, and wide-ranging applications. In this review, Si-based 3D microbatteries and related fabrication technologies, especially the production of micro-lithium ion batteries, are reviewed and discussed in detail in order to provide guidance for the design and fabrication.

Keywords three-dimensional (3D), wafer-scale, Si-based anode, micro-LIBs, thin-film deposition

1 Introduction

In recent years, the rapid development in integrated circuits (ICs) and micro/nano-electromechanical systems (M/NEMS) technologies have fast-tracked the commercialization of portable electronic devices and intelligent sensors [1–3]. According to the market forecasting made by the Yole Développement company of France (Fig. 1 [4]), future Si-based M/NEMS smart sensor devices, e.g., pressure sensing, gyroscope, micro-display, miniaturized thermal radiation tester, are expected to gain increasing revenue with wide applications in the fields of bio/medical engineering, military, finance, aerospace, intelligent communications/sensing, and so on. In these micro/nano-electronic devices, core components, such as micro-sensing, packaging, and software as well as the independent micro/nano-energy supply, are indispensable in achieving efficient power utilization.

Large capacity, high efficiency, small size, low heat loss, and long cycle life are required characteristics in an integratable micro (or even nano) power supply system. Feasible process integration and fabrication in a wafer-scale are also highly desirable. Recently, Si-based micro energy storage systems that are compatible with micro/nano-devices has drawn great interest among scientists engaged in research and development (R&D). Especially, three-dimensional (3D) Si-based micro-lithium ion batteries (micro-LIBs), embracing high energy/power density, excellent cycle stability, large operating condition range, easy miniaturization, etc., are considered as good candidates for miniaturized, integrated, and environmentally-friendly energy devices [5–8]. However, most of the Si-based 3D micro-LIBs still lack compatibility with current semiconductor processing technologies, and their corresponding electrochemical performance also needs further improvement.

This review focuses on the fabrication processes of 3D microbatteries and the influences of such processes on the respective electrochemical performances of the microbatteries. In the main context, we first review and compare the energy storage abilities of different electrochemical energy storage systems, followed by a specific introduction of the working principles and applications of micro-LIBs. Then, the historical development of micro-LIBs from 2D to 3D configurations is introduced and the different types of 3D micro-LIBs are summarized. Subsequently, we presented the advantages of 3D Si-based micro-LIBs with emphasis on various structures of micro/nano-electrodes. Finally,

Received February 9, 2017; accepted May 8, 2017

Chuang YUE, Jing LI (✉)
Collaborative Innovation Center for Optoelectronic Semiconductors and Efficient Devices, Pen-Tung Sah Institute of Micro-Nano Science and Technology, Xiamen University, Xiamen 361005, China
E-mail: lijing@xmu.edu.cn

Chuang YUE, Liwei LIN
Department of Mechanical Engineering, University of California, Berkeley, CA 94720, USA

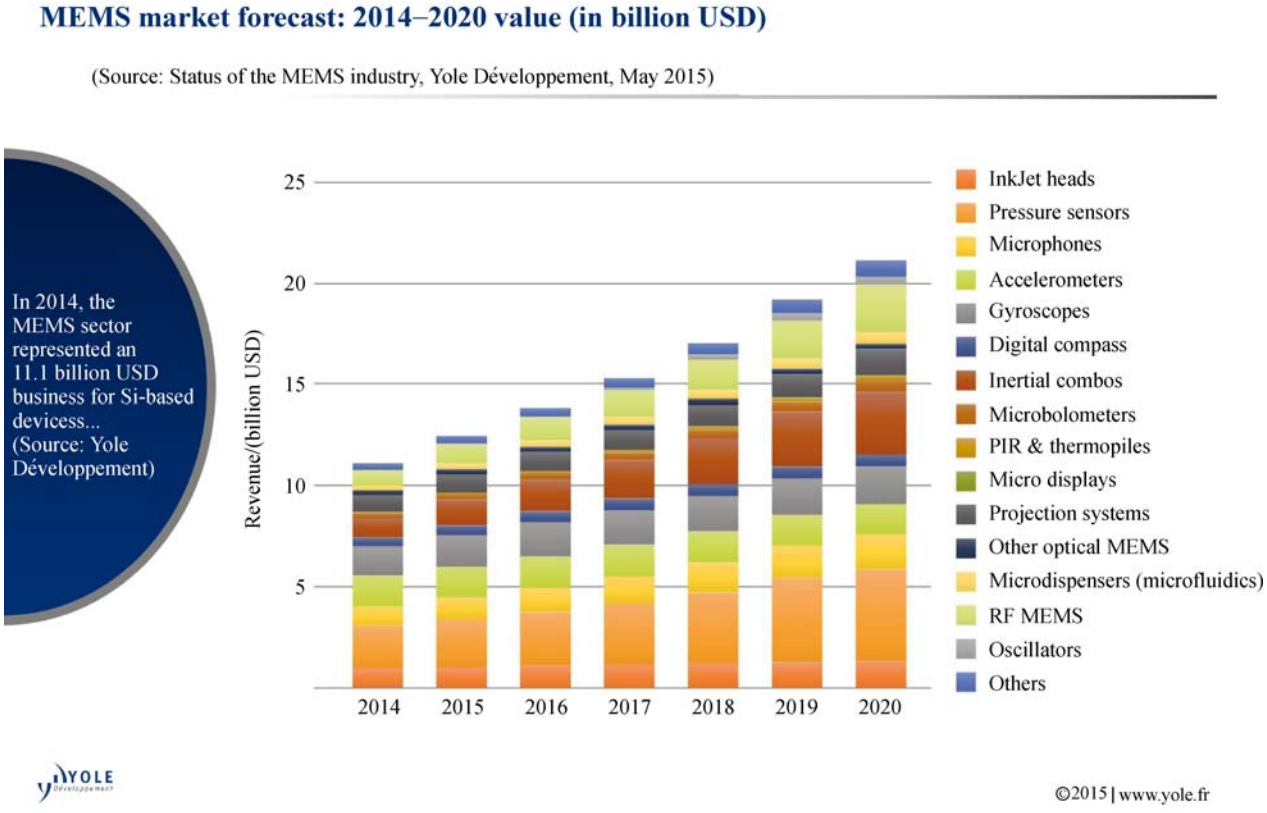

Fig. 1 Market forecasting of the different Si-based MEMS smart devices in the future [4]

recently fabricated 3D Si-based micro-LIBs via diversified technologies are classified and discussed.

2 Micro energy storage systems

A micro energy system is a micro-device that can convert different energies into electrical energy. Depending on its energy sources, the micro energy system can be classified as rechargeable micro-LIBs [9], solar cells [10], micro nuclear batteries [11], micro-fuel cells [12] and micro-thermoelectric batteries [13]. Among them, the micro-LIB, as an electrochemical energy storage source based on the principle of LIBs which has higher energy density (Fig. 2 [14]), mature preparation technology, and a wider range of operating temperatures and intensive commercial applications, is definitely a good candidate for a micro-power supply system. Moreover, the all-solid-state micro-LIB processing presents possible compatibility with smart micro/nanoelectronic devices.

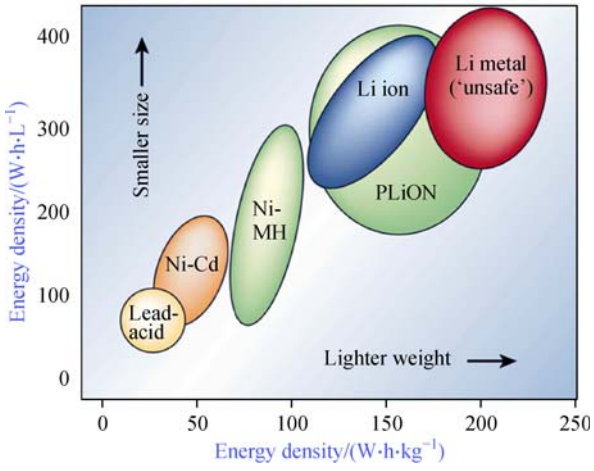

Fig. 2 Ragone plot of different electrochemical energy storage systems. Reprinted with permission from Ref. [14]. Copyright 2001, Nature Publishing Group

2.1 Working principle and application of micro-LIBs

Similar to traditional LIBs, micro-LIBs consist of an anode (negative), cathode (positive), separator, electrolyte, and current collectors for repeated charging/discharging processes. As shown in Fig. 3 [15], oxidation/reduction reactions occur in the electrodes during the working cycles.

The reactions in the graphite anode (negative electrode) and $LiCoO_2$ cathode (positive electrode) are described in Fig. 4.

During the charging process, the Li ions are released

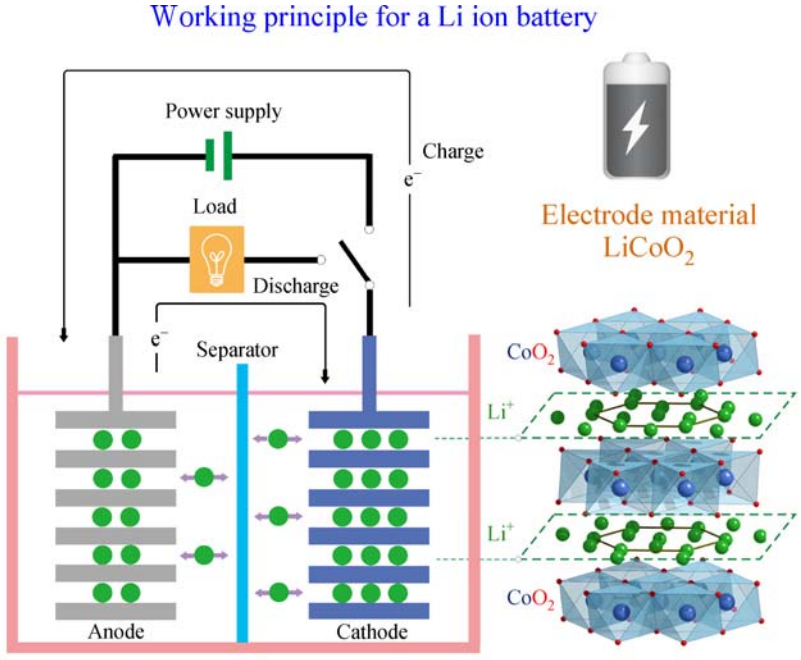

Fig. 3 Illustration of the working principle of a Li-ion battery [15]

$$\text{(−) Anode: } xLi^+ + 6C + xe^- \underset{\text{Discharge}}{\overset{\text{Charge}}{\rightleftharpoons}} Li_xC_6 \quad (1)$$

$$\text{(+) Cathode: } LiCoO_2 \underset{\text{Discharge}}{\overset{\text{Charge}}{\rightleftharpoons}} xe^- + xLi^+ + Li_{1-x}CoO_2 \quad (2)$$

Fig. 4 Reactions that occur in the electrodes of a Li-ion battery during the charge/discharge process [15]

from the $LiCoO_2$ positive electrode, and then inserted into the graphite negative electrode through the electrolyte. Meanwhile, the electrons are transferred from the positive to the negative electrode through the external circuit, before they eventually recombine with the Li ions. Meanwhile, the opposite processes occur during the discharging process [15,16].

Currently, LIBs can be fabricated in varying sizes for different areas according to the energy storage capability. As shown in Fig. 5 [17–28], the capacity in the μW·h–mW·h range is ascribed to a micro-LIB unit and can power the micro/nano smart devices. The overall capacity of the micro-LIB is much less than that of a battery for applications in portable electronics (W·h) and the electric vehicles (kW·h). In recent years, the all-solid-state thin-film LIB, with thickness of about 170 μm and up to thousands of working cycles has been successfully produced by the US company, ThinEnergy, making it the only commercialized microbattery at that time [18].

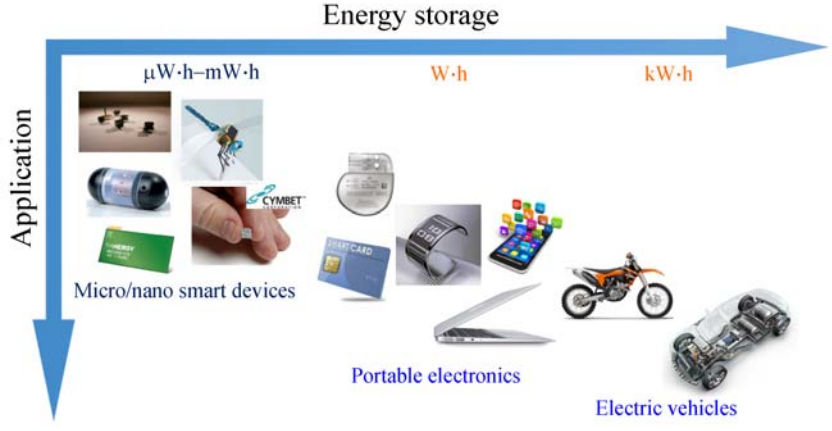

Fig. 5 Applications of different Li-ion battery energy storage systems [17–28]

Another US company, Cymbet, fabricated the wafer-scale all-solid-state Li-ion micro-secondary battery, which can be integrated with the smart IC chips with the minimum current density supply in the $nA \cdot cm^{-2}$ order of magnitude [19]. However, the electrochemical performances of the current micro-LIBs require further improvement and a mass production process to guarantee its commercialization. Therefore, conducting further research on integratable and high-performance micro-LIB energy storage systems is highly significant.

2.2 Structural evolution of micro-LIBs from two-dimension to three-dimension

2.2.1 Development of the three-dimensional micro-LIBs

Due to the successful development of the solid-state electrolytes, it is now possible to realize, solidify, miniaturize, and commercialize micro-LIBs. Traditionally, micro-LIB energy storage systems have a two-dimensional (2D) thin-film structure. For example, Figs. 6(a) and 6(b) [29,30] show thin-film all-solid-state LIBs with a 2D sandwich structure (–) Li/LiPON/Li_2MnO_4 (+). In the microbattery, the overall footprint area and thickness are about 3 mm^2 and 15 μm, respectively. The energy and power densities of a cell are tens of $\mu A \cdot h \cdot cm^{-2}$ and $\mu W \cdot cm^{-2}$. Normally, the overall volume of the microbattery is small, and the mass of the active material is difficult to measure accurately, such that the energy and power density are expressed in $\mu/mA \cdot h \cdot cm^{-2}$ and $\mu/mW \cdot cm^{-2}$ [31,32]. Intrinsically, as shown in Fig. 6(c), both the energy and power densities of a 2D thin-film LIB cannot be increased simultaneously by only controlling the thickness of the electrode material in a limited footprint area. However, in the novel 3D battery structure, the areal Li-ion inserting capacity can be increased due to the enlarged specific surface area and the more active material used in the same footprint area. Moreover, the power density can be improved because of the relatively short Li-ion diffusion distance. Consequently, both the energy and power density can be improved in 3D microbattery systems [30].

Generally, as shown in Fig. 7 [33–36], the fabrication of 3D micro-LIBs is mainly based on the battery's key components, namely, the current collector, electrode materials, and the electrolyte. The details are given below.

1) 3D current collector preparation. Typically, a conductive substrate, such as Cu [37], Ti [38], or C [39], is used as the substrate. For example, as shown in Fig. 7(a), researchers used a porous anodic aluminum oxide as a template to fabricate the 3D Al nanocolumnar arrays by electroplating, which benefited the rapid electron transfer in the battery. Subsequently, the TiO_2 thin-film anode material was prepared by atomic layer deposition (ALD) technology, and a total areal capacity of about 0.01 $mA \cdot h \cdot cm^{-2}$ was obtained [33].

2) 3D electrode material fabrication. This methodology is employed in processing materials, such as Si [40], Ge [41], TiO_2 [42], and $LiCoO_2$ [43]. It is the most commonly used experimental procedure to improve the electrochemical properties of a battery. As shown in Fig. 7(b), the 3D Si nanopillar array electrode was produced by the glancing angle deposition (GLAD) technique [37]. Compared with the 2D solid-state dense silicon thin-film electrode, both the areal capacity (90 vs. 40 $\mu A \cdot h \cdot cm^{-2}$) and the rate performance of the 3D Si electrode were all significantly improved [34].

3) 3D electrolyte structure construction. As an example shown in Fig. 7(c), Yoshida et al. [35] (NGK Insulators Limited, Japan) synthesized a double-sided, honeycomb, solid electrolyte $Li_{0.35}La_{0.55}TiO_3$ (LLT) using a template method. The contact areas of the ($LiCoO_2$) negative and ($Li_4Mn_5O_{12}$) positive electrode were increased, thus the electrochemical performance of the battery was improved.

4) 3D integrated battery construction. Recently, as

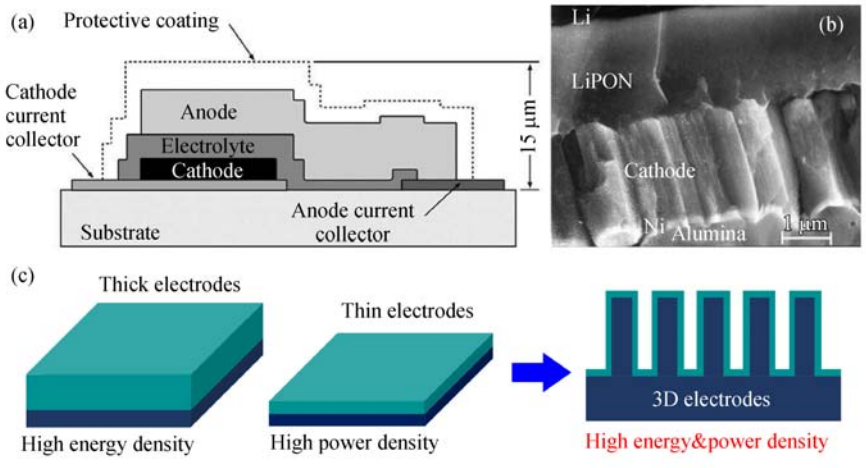

Fig. 6 (a) Diagram of a conventional 2D all-solid-state thin-film Li-ion battery structure and (b) its SEM section view. Reprinted with permission from Ref. [29], Copyright 2000, Elsevier. (c) Advantages of the 3D battery structure [30]

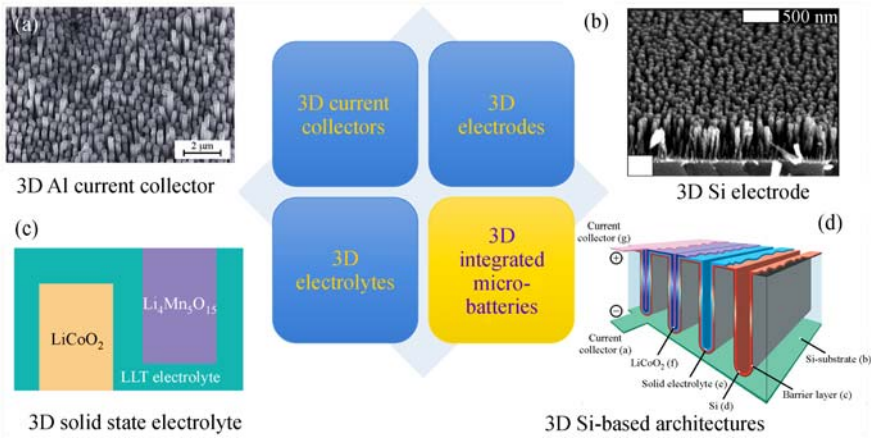

Fig. 7 Different structures of 3D micro-LIBs. (a) 3D Al current collector. Reprinted with permission from Ref. [33], Copyright 2009, American Chemical Society. (b) 3D Si electrode. Reproduced with permission from Ref. [34], Copyright 2013, Wiley-VCH. (c) 3D solid state electrolyte based on Ref. [35]. (d) 3D Si-based architectures. Reproduced with permission from Ref. [36], Copyright 2007, Wiley-VCH

shown in Fig. 7(d), the 3D Si-based micro-LIB structure was successfully fabricated by Peter H. Notten's group [36] at the Eindhoven University of Technology in Netherlands. The TiN and the amorphous Si (thickness ~50 nm) thin-film layers were employed as the Li-ion barrier layer and anode material, respectively. In half-cell testing, the 3D Si-based electrode delivered an areal capacity of about 40 $\mu A \cdot h \cdot cm^{-2}$ after 150 cycles [36].

Although the three methods mentioned above can improve the energy and power densities of the micro-LIBs, the fact that the fabrication process is less compatible with the traditional semiconductor Si technology remains a significant issue in this field. Moreover, a more simplified preparation process and reduced manufacturing costs are expected. To solve these problems, the Si-compatible technology developed by Peter H. Notten's group [36] has shown potential in the preparation of 3D integratable micro-LIBs. However, challenges still exist because the battery fabrication process involves a complex lithography process, and the overall electrochemical performance, especially the cycling performance, still needs to be further improved. Therefore, developing compatible, low-cost, simple, and reproducible fabrication technologies for the production of high-performance 3D integratable micro/nano-LIBs remains an immediate task.

2.2.2 Advantages of Si in three-dimensional micro-LIBs

The electrochemical energy storage ability of micro-LIBs not only depends on the electrode structure, but also on the electrode materials. The materials in LIBs (including anodes, cathodes, and electrolytes) have been investigated in many past studies with great progress. Further, with the consideration of the compatibility of the battery fabrication process and integratibility with the micro/nanodevices, Si-based micro-LIB energy storage systems have been shown to have several exceptional advantages compared with others (Fig. 8 [44–47]), as enumerated below.

1) First, the Si material is abundant in nature and is not a significant pollutant to the environment. Moreover, as shown in Fig. 8(a), the Si electrode itself, as an LIB anode material, has excellent electrochemical properties, e.g., lower relative potential ($\leqslant$0.5 V vs. Li/Li^+) and higher Li-ion storage ability ($Li_{3.75}Si$-3572 $mA \cdot h \cdot g^{-1}$) at room temperature [44], equivalent to more than ten times of the current commercially produced graphite material (LiC_6-376 $mA \cdot h \cdot g^{-1}$).

2) Second, from the battery structural aspect, as shown in Fig. 8(b), the complex 3D Si-based microchip structures are primarily based on mature semiconductor Si-processing technologies [45]. Therefore, different kinds of 3D Si-based micro-LIB structures can be easily fabricated by the Si-processing technology, and the corresponding electrochemical properties can also be greatly enhanced.

3) Again, as shown in Fig. 8(c), a wafer-scale micro/nano-LIB cell can facilitate the integration of the micro-power supply module with other micro/nano-smart devices on a single chip [46,47].

4) Finally, all the components of the Si-based micro-LIB, including the solid-state electrolyte, positive and negative electrode materials, etc., can be fabricated consecutively by the microelectronic thin-film deposition process. Therefore, by using the Si electrode material and the corresponding Si-based semiconductor technology, the wafer-scale 3D Si-based micro-LIBs can be produced together with micro/nano-electronic devices.

Unfortunately, apart from the abovementioned extraordinary properties, the Si anode material generally experiences a large volume expansion (~300%) during the repeated charging/discharging process. As shown in Fig. 9(a) [48], electrode pulverization or detachment from the bottom current collector often happens after cycling in

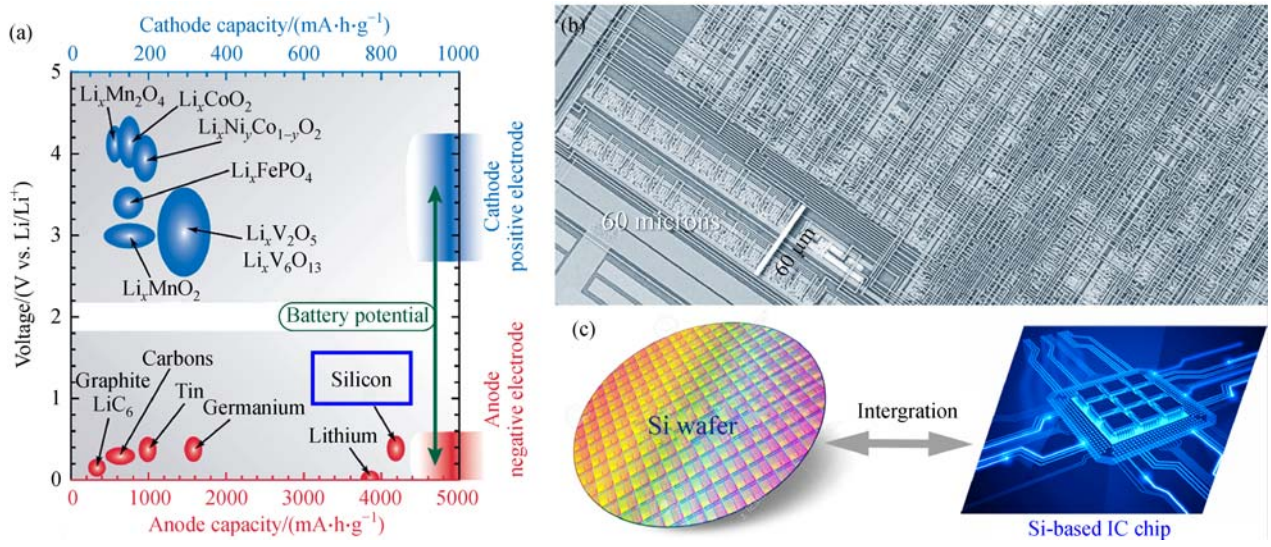

Fig. 8 (a) Theoretical capacity and relative potential vs. Li/Li$^+$ of common electrodes in LIBs. Reprinted with permission from Ref. [44], Copyright 2009, Royal Society of Chemistry. (b) Scanning electron microscopy (SEM) image of the complex Si-based microchip structure; (c) wafer-scale LIB units can be potentially integrated with the micro/nano-intelligent electronic devices [45–47]

LIBs that use 2D Si thin-film or Si nanoparticle as anodes, thus resulting in the poor electrochemical performance of batteries. Therefore, in recent years, many researchers have focused on solving the issue of large volume expansion in Si electrodes. For example, as shown in Fig. 9(a), 3D silicon nanowire anodes, prepared by metal-catalyzed (Au) chemical vapor deposition (CVD) technique are used to address the volume change issue [48]. Based on the literature, two common approaches can be employed to address the volume expansion issue.

1) From the structural aspect

This approach is used in fabricating the 3D micro/nano-structured Si electrodes, e.g., nanowires, nanotubes, hollow nanospheres, as shown in Figs. 9(b)(i) [48–51]. Structurally, the sufficient space provided by the 3D configuration is helpful in buffering/retarding volume expansion and in reducing stress in the Si electrode. Furthermore, the current polarization effect in the working electrode can be reduced due to the increased active surface area in low-dimensional structures. Moreover, the diffusion path of lithium ions can be understandably shortened, thus leading to the improved stability in Si anodes.

2) From the material aspect

This approach is used in fabricating 3D Si-based nanocomposite electrodes, as displayed in Fig. 9(b)(ii) [52–55], such as the Si/C nanocomposite particles, Si/Ge, Si/C nanotubes, Si/Graphene. This kind of nanocomposite acting as electrodes has several advantages. First, the 3D nanocomposite shell electrode not only provides extra reversible sites for Li-ion insertion/extraction and further increases the whole areal capacity of an electrode, it also helps improve the surface electronic/ionic conductivity, thus promoting the electrochemical kinetics process in the Si electrode. Second, the nanocomposite thin-film can effectively prevent direct contact between the Si electrode and the electrolyte, thus reducing the continuous generation of the solid electrolyte interphase (SEI) layer. Therefore, aside from the largely buffered or restricted volume expansion, the improved electrochemical performance can also be accomplished in the Si electrodes with various composite components.

However, currently, most of the Si-based nanocomposite or micro/nano-structured anodes are either bulk materials (the mixture of the carbon black, binder, and Si-based active materials) or directly fabricated on the metal substrates, which are quite challenging for the battery miniaturization, integration, and packaging with the micro/nano-device. In comparison, the wafer-scale 3D Si-based nanocomposite electrodes present possible compatibility and integratibility with the micro/nano-devices and promising electrochemical properties. The recent advances in wafer-scale 3D Si-based integrated micro-LIBs shall be discussed in two directions: Si substrate serving as the 3D supporting structure, and the 3D-patterned Si substrate acting as both the supporting structure and the active electrode material.

3 Fabrication of three-dimensional Si-based micro-LIBs

3.1 Three-dimensional micro-LIBs with Si as a supporting structure

When the Si substrate only serves as the supporting structure, a barrier interlayer, such as TiN [56], Pt [57], SiO_2 [58], Al_2O_3 [59], is normally employed to block the

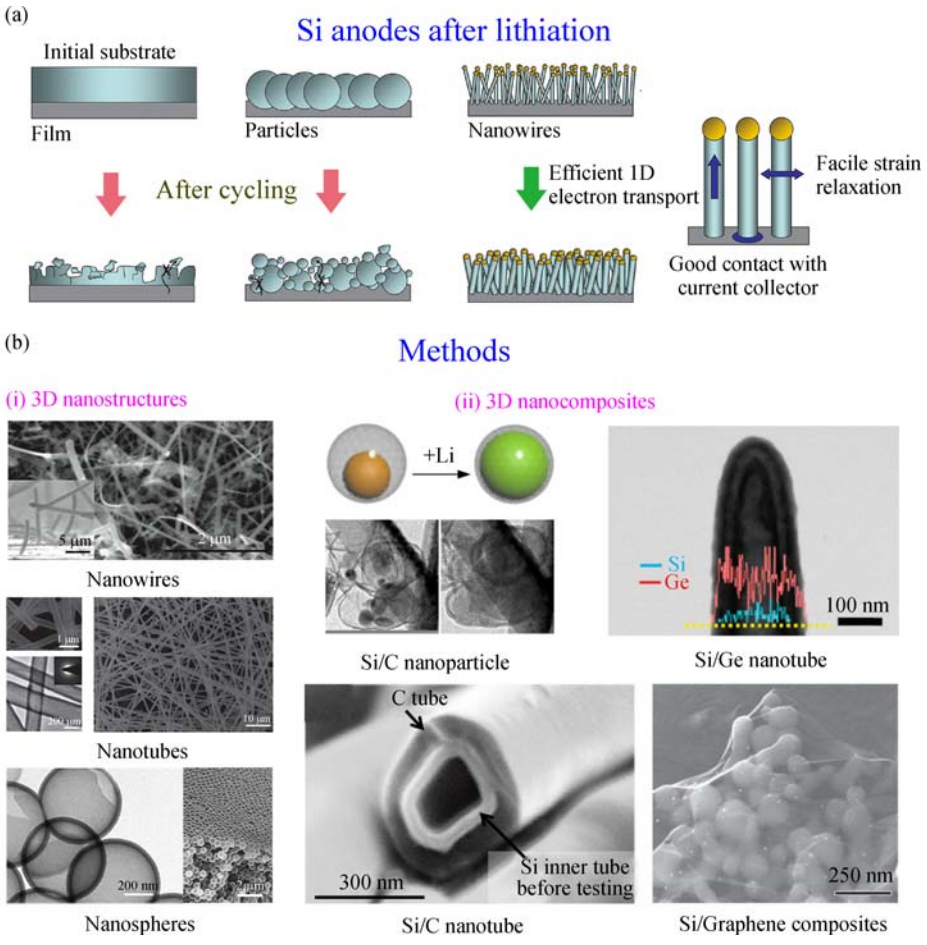

Fig. 9 (a) Schematic illustration of different Si anode morphology changes after lithiation process. Reprinted with permission from Ref. [48], Copyright 2007, Nature Publishing Group. (b) The two main methods used to solve the issue of large volume expansion in Si electrodes. Reprinted with permission from Refs. [48,49], Copyright 2007/2012, Nature Publishing Group; reprinted with permission from Refs. [50,52–54], Copyright 2011/2012/2012/2011, American Chemical Society; reproduced with permission from Ref. [55], Copyright 2014, Wiley-VCH

insertion of Li ions into the Si substrate and reduce the interference to other integrated electronic devices. Based on the type of electrolyte applied in a battery, researchers carried on their works mostly on either a half-cell unit or a full-battery unit.

3.1.1 Half-cell unit

As in Notten's concept of 3D, integrated all-solid-state micro-LIBs (Fig. 10(a) [60]), the 3D Si geometries (in depths of 10–100 μm) including micro trench or pillar arrays, were first prepared by the traditional Si dry-etching technologies. Then, the subsequent Li-ion barrier layer and other key components were sequentially deposited onto the 3D patterned Si surface. As seen in Figs. 10(b)–10(d), the TiN barrier layer and the poly-Si electrode were successfully coated on the 3D Si trench with different aspect ratios (AR, 10 and 20) by the atomic layer deposition (ALD) and low pressure chemical vapor deposition (LPCVD) methods, respectively. Obviously, all thin films located in the top surface were much more conformal and thicker than those in the middle or bottom parts of the 3D Si structure. Subsequently, as shown in Fig. 10(e), the cycling performance of the above two kinds of 3D Si/TiN/poly-Si stack electrodes were then performed at a current density of 25 $\mu A \cdot cm^{-2}$ within a voltage window between 0 and 3.0 V vs. Li/Li^+. Both the 3D electrodes experienced a drastic capacity drop only after 20 cycles. This can be attributed to the filling of the porous and thick solid electrolyte interphase (SEI) layer in the space of the electrode (AR 10), as seen in Figs. 10(f) and 10(g), which was formed only after 10 cycles and continuously expanded afterwards. The application of an extra-solid-state LiPON electrolyte layer can well promote the electrochemical kinetics by restricting the growth of SEI layer, resulting in a greatly enhanced cycling performance in corresponding electrodes [61,62].

Furthermore, Notten's group [63] also fabricated the 3D

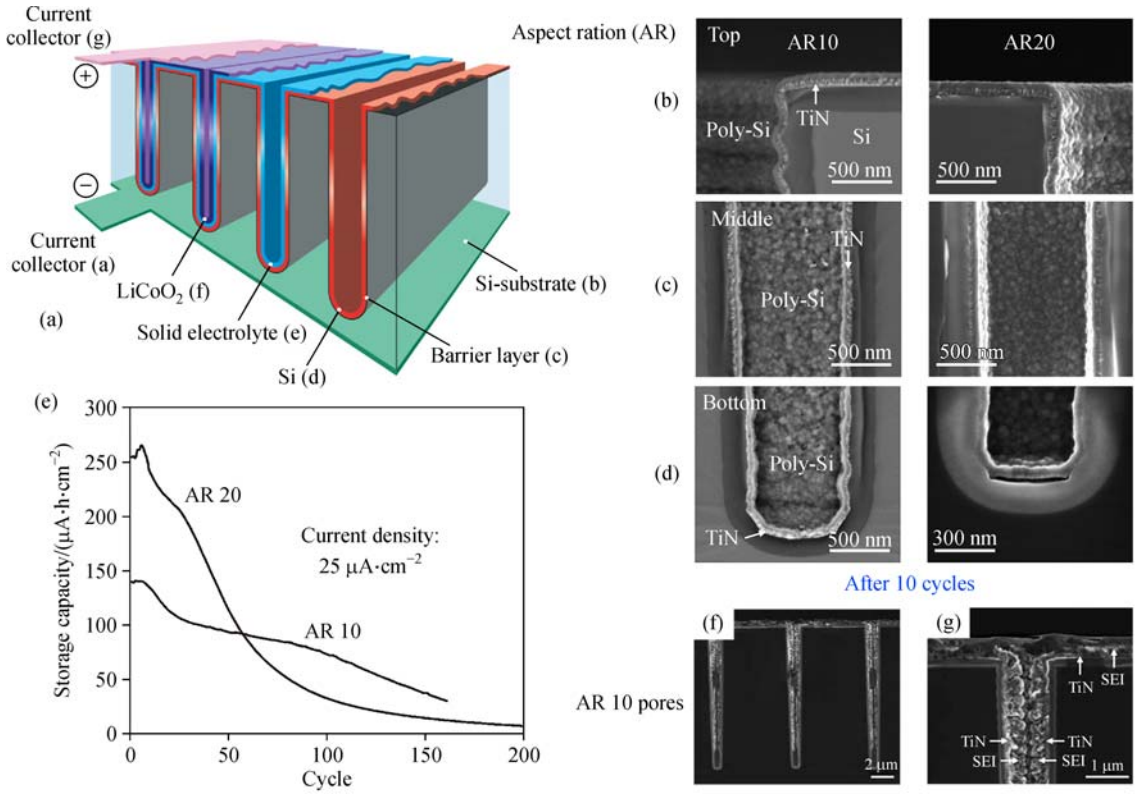

Fig. 10 (a) Scheme of 3D integrated all-solid-state micro-LIB. Reproduced with permission from Ref. [36], Copyright 2007, Wiley-VCH. (b)–(d) SEM images of different locations in 3D Si/TiN/poly-Si electrodes (AR 10 and 20); (e) the cycle performance of the 3D TiN/poly-Si stacks (AR 10 and 20) at a current density of 25 $\mu A \cdot cm^{-2}$ within a voltage window from 0–3 V vs. Li/Li^+; (f)–(g) SEM images of the 3D Si/TiN/poly-Si electrode (AR 10) after 10 charge/discharge cycles. Reprinted with permission from Ref. [60], Copyright 2010, Royal Society of Chemistry

Si/TiN/Pt/TiO_2 stack electrodes (Si pillar: Diameter, 1 μm; height, 30 μm). Both the TiN Li-ion barrier layer and Pt thin-film current collector were prepared by the ALD method. Afterwards, the uniform TiO_2 thin-film was deposited by the LPCVD technique at a temperature of 350 °C. The condensed TiN thin interlayer can effectively buffer the Li-ion insertion into the 3D Si substrate. However, the areal capacity of this kind of 3D integrated micro-LIBs is low. In this manner, the 3D all-solid-state full-battery fabrication process, especially the solid-state electrolyte conformal deposition, should be further accomplished and optimized [63].

Interestingly, another group also employed the compatible microelectronic facilities to produce the 3D novel scaffold microtubes on the Si-wafer [64]. As shown in Fig. 11(a), this kind of 3D Si-based supporting structure can provide adequate space within the microtubes. Moreover, the surface area was further increased in the mechanically robust 3D Si microtube structures with optimized depth-to-width ratio. As displayed in Figs. 11(b)–11(d), the current collector and active anode material were successfully produced by the subsequent conformal deposition of Pt and anatase TiO_2 thin-films using the ALD technique. By employing the standard liquid electrolyte, as displayed in Figs. 11(e) and 11(f), the best electrochemical kinetics and Li-ion storage abilities were accomplished in the 3D Si/Pt/TiO_2 microtube anodes compared with the 2D planar Si/Pt/TiO_2, and even the 3D Si/Pt/TiO_2 micropillar electrodes. Therefore, an improved electrochemical performance could be expected in micro-LIBs by using these novel 3D Si microtubes as an effective supporting structure.

In order to further increase the surface area, as shown in Figs. 12(a) and 12(b), Eustache et al. [65] optimized the experiment design and fabricated the 3D Si double microtubes on the Si wafer. The fabrication process also used the photoresist as the template and the inductive coupled plasma (ICP) Si dry etching technologies. Afterwards, the Al_2O_3/Pt/TiO_2/Li_3PO_4 stacking layers (~100 nm-thick) were then step-deposited on the 3D Si patterns by using the ALD technique [65]. As displayed in Figs. 12(c)–12(f), the stacking layers were conformal and compact on the 3D Si pattern surface. From Fig. 12(g)–12(l), the corresponding element mapping also showed the Si-3D/Al_2O_3/Pt/TiO_2/Li_3PO_4/SiO_2 stacked functional layers in a close contact. The Li_3PO_4 solid-state electrolyte layer, located in between the TiO_2

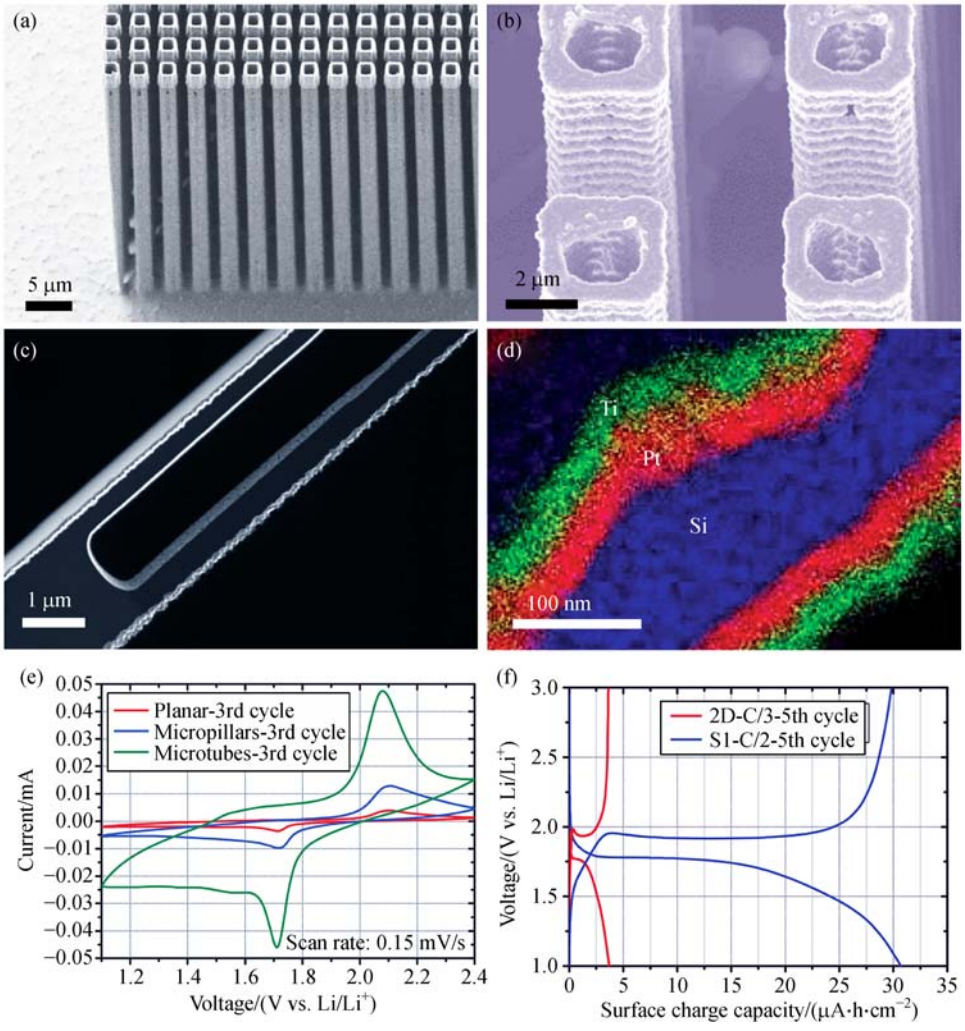

Fig. 11 SEM images of the (a) Si/photoresist microtubes and (b) Si/Pt/TiO_2 microtubes after the etching mask removal, ALD of Pt and TiO_2; (c)–(d) scanning transmission electron microscopy (STEM) image of a single Si/Pt/TiO_2 microtube and the energy-dispersive X-ray spectroscopy (EDX) elemental mapping for Ti, Si, and Pt elements; (e) cyclic voltammetry (CV) measurement results of the 2D planar, micropillars, and microtubules electrodes decorated with the Pt/TiO_2 layers; (f) gavalnostatic charge/discharge testing for the 2D (TiO_2 layer, 60 nm) and 3D Si/Pt/TiO_2 microtube electrodes (S1 samples: TiO_2 layer, 60 nm). Reproduced with permission from Ref. [64], Copyright 2014, Wiley-VCH

and SiO_2-protective layers, could not be detected using the EDX probing. As shown in Fig. 12(m), the high-resolution transmission electron microscopy (HRTEM) image further verified the close contact in the multilayers. In addition, the inset lattice distance can be attributed to the (011) plane of anatase TiO_2, which is identified as the highly crystalline TiO_2 layer. The fabricated 3D Li_3PO_4 pinhole free solid-state electrolyte has a thickness of 10 nm, which can increase the Li-ion source and subsequently enhance the surface capacity. Finally, after the subsequent electrochemical testing in the liquid electrolyte, as shown in Figs. 12(n) and 12(o), the 3D Si-3D (simple microtube)/Al_2O_3/Pt/TiO_2/Li_3PO_4 multilayer anodes displayed improved surface capacity and good rate performance. Thus, the two abovementioned 3D Si-based electrodes can effectively increase the surface area and achieve improved electrochemical performances in the corresponding micro-LIBs.

Another method can be used to fabricate the 3D Si-based micro-LIBs using the 2D planar Si substrate as the supporting structure. Gerasopoulos et al. [66] successfully fabricated 3D Au micropillar current collectors on the planar Si substrate. Both the SiO_2 and Cr/Au thin-films were employed as the Li-ion barrier layers. As shown in Figs. 13(a) and 13(b), the 3D Au micropillar arrays were prepared by the electroplating technique, and the 3D photoresist pores were employed as the electroplating mode. The novel hierarchical 3D Si/SiO_2/Cr/Au-3D/TMV (Tobacco mosaic virus, templates)/Ni electrodes were obtained by the solution method, so that the surface

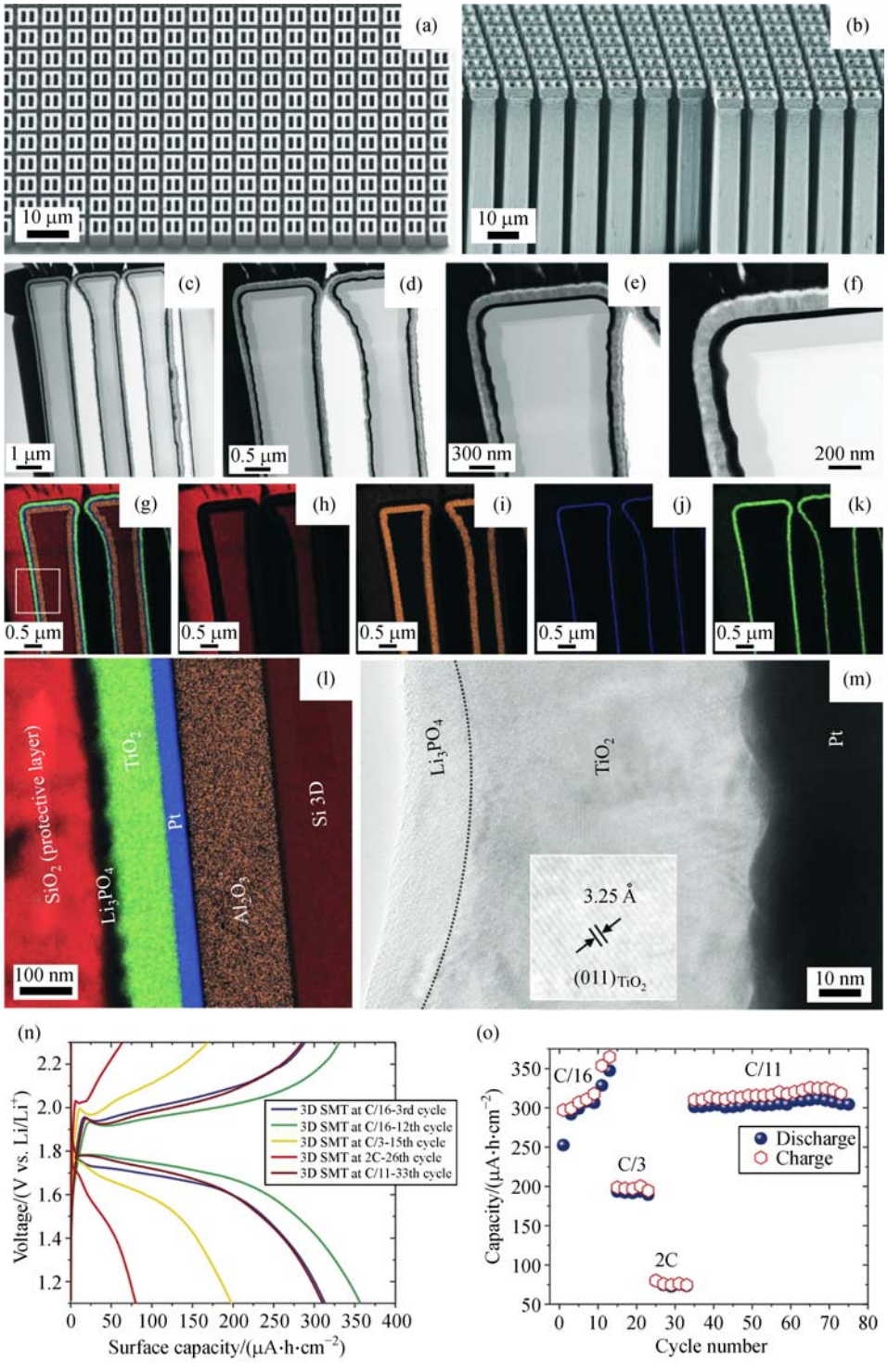

Fig. 12 (a)–(b) SEM images of the fabricated Si double microtubes before and after the removal of photoresist mask using the deep reactive ion etching technique; (c)–(f) different magnification TEM images of Al_2O_3/Pt/TiO_2/Li_3PO_4 stacking layers coated on the 3D double microtubes; (g)–(l) EDX-STEM elemental mapping of the Si-3D/Al_2O_3/Pt/TiO_2/Li_3PO_4/SiO_2-protective stacked layers; (m) high-resolution transmission electron microscopy (HRTEM) image of the Pt/TiO_2/Li_3PO_4 layers; (n)–(o) the differential surface capacity versus potential plots and the rate performance of the Si-3D (simple microtube: SMT)/Al_2O_3/Pt/TiO_2/Li_3PO_4 electrodes. Reproduced with permission from Ref. [65], Copyright 2016, Wiley-VCH

area was further increased. Afterwards, as shown in Figs. 13(c)–13(e), the micro-LIB anode material (V_2O_5) was uniformly deposited on the 3D hierarchical micro/nano-networks by the ALD technique. Therefore, the micro (Au pillars) and nano (TMV forests template) components were co-presented in the 3D micro-LIB electrodes. As seen in Figs. 13(f) and 13(g), the hierarchical $Si/SiO_2/Cr/Au$-3D/TMV/Ni/V_2O_5 micropillar electrodes demonstrate enhanced electrochemical performance. Moreover, the energy/power density can also be further improved by depositing other active materials with higher specific capacities into these 3D micro/nano-supporting structures or by fabricating 3D battery supporting micro structures with higher aspect ratios. However, the areal capacity and the adhesion ability of the 3D metal current collector to the Si substrate must be improved. Briefly, the supporting structure patterned on the 2D Si-wafer surface is favorable in improving the energy storage performance of a 3D micro-LIB.

3.1.2 Full-cell unit

The aforementioned 3D Si-based micro-LIBs liquid electrolytes were generally used to facilitate the half-cell assembling and testing. The liquid electrolyte and Li metal electrode-based LIB may suffer from leakage or may short circuit, which are major safety concerns [67,68]. Herein, we reviewed recent advancements in 3D Si-based full

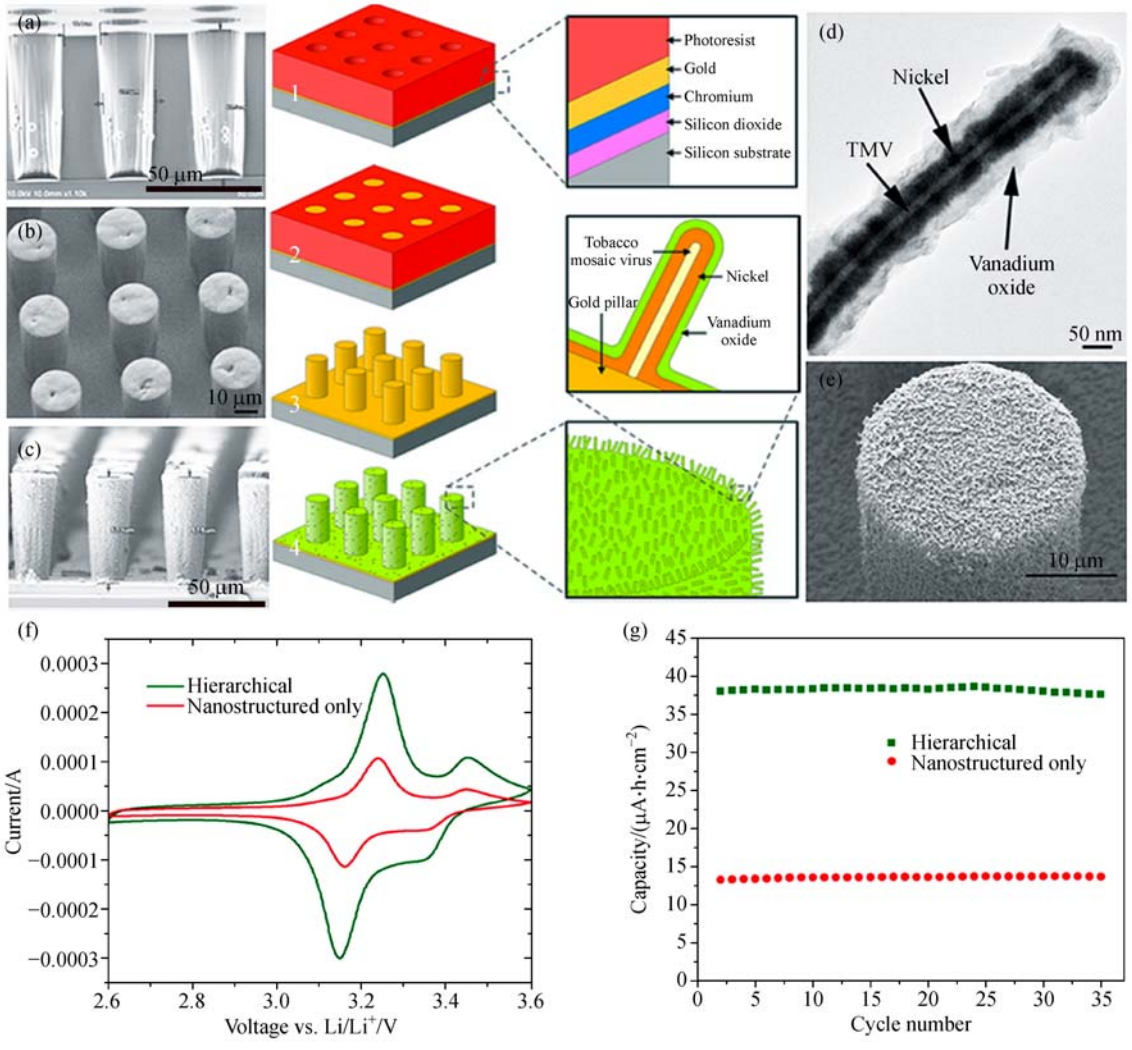

Fig. 13 (a) SEM image of the photoresist mold patterned on the Si wafer; (b) SEM image of the 3D Au current collector employing electroplating followed by the mold removal; (c) SEM image of the Tobacco mosaic virus (TMV) nanostructures self-assembled onto the 3D gold micropillars surface and then coated with Ni thin-film in an electroless plating solution, followed by ALD of V_2O_5 anode; (d) TEM image of an individual virus-templated nanorod; (e) SEM image of a single Si/Au-3D/TMV/Ni/V_2O_5 micropillar in a close-up top view; (f) CV measurement and (g) cycle performance of the virus-structured electrodes with and without 3D Au micropillars; (1)–(4) Scheme of the Si/Au-3D/TMV/Ni/V_2O_5 micropillar electrodes fabrication process. Reproduced with permission from Ref. [66], Copyright 2012, American Chemical Society

micro-LIBs and their corresponding processing technologies.

As shown in Figs. 14(a) and 14(b) [69–71], Nathan and co-workers first reported the production of battery supporting structures for 3D micro-LIBs using a process compatible with current Si-based semiconductor technologies. The full 3D microbattery was manufactured on the perforated Si substrate by using the wet chemistry method. Thousands of high-aspect-ratio holes per square cm exist in the Si wafer and thus, the surface area per given footprint can be increased by at least more than one order of magnitude. Then, the conformal thin-film electrodes, electrolytes, and current collectors were sequentially deposited on all available surfaces of the 3D Si substrate. Here, the cathode current collector (nickel), cathode (MoS_2), and the hybrid polymer electrolyte (HPE) were prepared by employing the electrodeless, solution, and electrodeposition methods, respectively. A lithiated graphite slurry simultaneously served as the anode and the anode current collector. As depicted in Fig. 14(c), the 3D full micro-LIB had significantly greater capacity than the 2D planar thin-film micro-LIB at the same footprint area and electrode thickness. Nevertheless, the conformal deposition of the battery materials and the final double side microbattery packaging are still major challenges that must be overcome. Moreover, alternative strategies are still needed in order to simplify the fabrication process of a whole microbattery, especially the electrolyte, as well as to address the compatibility issue.

Another interesting approach has been reported, in which the 3D interdigitated carbon/polypyrrole (PPY) micro-LIB electrode arrays were generated by using the carbon-MEMS (C-MEMS) technology [72]. In this method, the spacing and geometry of the electrode can be well controlled in a 3D configuration, which also exhibited improved electrochemical properties compared with the 2D ones. As shown in Fig. 15(a), the fabrication process involved depositing the SiO_2 interlayer as the Li-ion barrier layer to the 2D planar Si substrate; then, the 3D interdigitated C micropillar current collector arrays were formed after completing the traditional lithography and pyrolysis process. Afterwards, the cathode dodecylbenzenesulfonate-doped polypyrrole (PPYDBS) thin-films were coated onto one of the 3D C current collector arrays using the electrochemical deposition method. Another group of C micropillar arrays acted as both the anode and anode current collector. As displayed in Figs. 15(b) and 15(c), the 3D interdigitated C/PPYDBS electrode arrays were

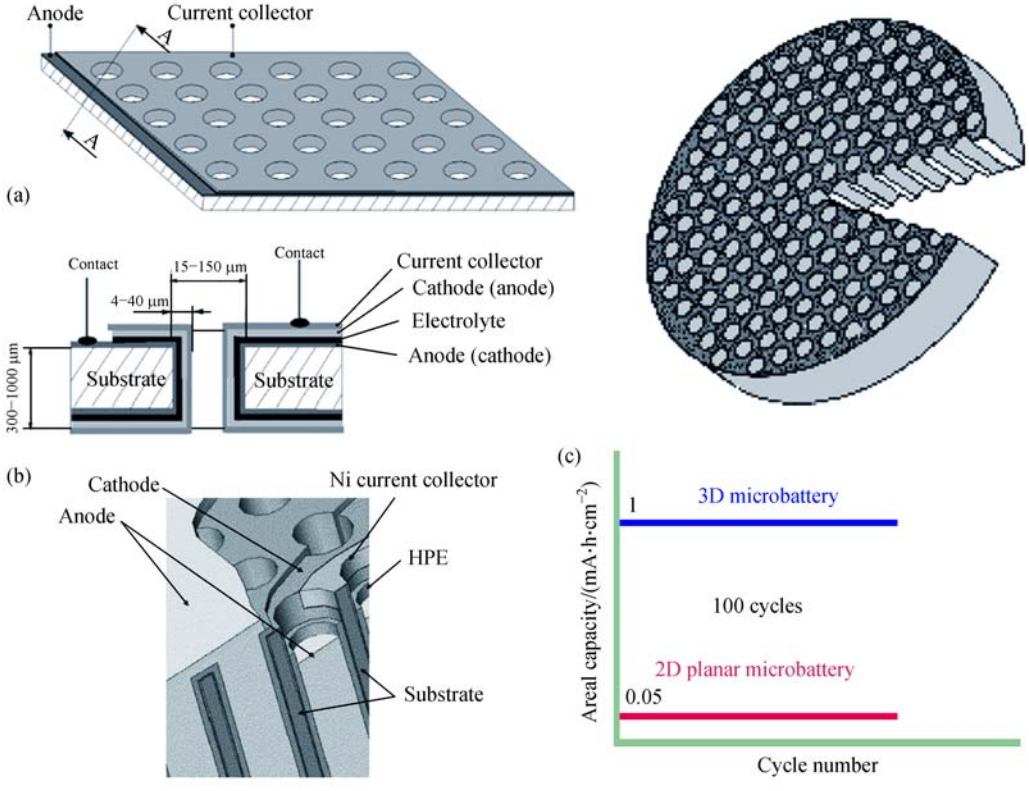

Fig. 14 (a)–(b) Schematic description of a 3D micro-LIB on a perforated Si or glass substrates. Reproduced with permission from Refs. [69,70], Copyright 2005/2006, Elsevier. (c) Comparison of the areal capacity between the 3D micro-LIB and 2D thin-film micro-LIB. Data based on Ref. [71]

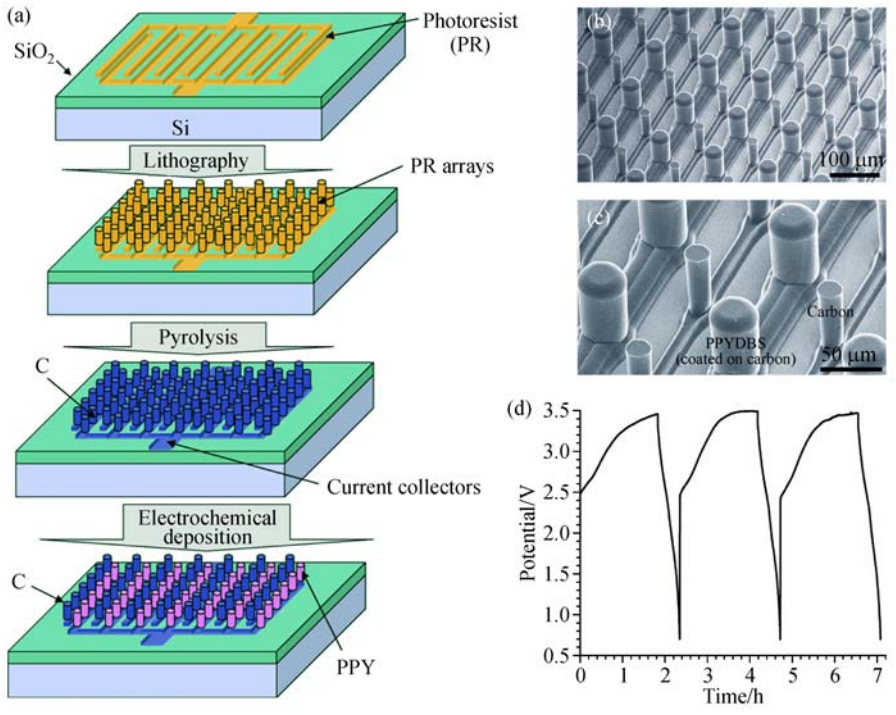

Fig. 15 (a) The fabrication process of the 3D micro-LIB; (b)–(c) SEM images of C/PPYDBS interdigitated electrode arrays and (d) its charge/discharge characteristic. Reproduced with permission from Ref. [72], Copyright 2007, Elsevier

periodically and vertically standing on the Si substrate. However, there was an operation limit, as shown in Fig. 15(d), in which the whole battery displayed electrical shorting phenomenon when the charging time was much longer than the discharging time. Moreover, the Li-ion conduction medium was still in the liquid electrolyte. Despite its limitations, this novel and meaningful work paved the way for the design and optimization of future 3D Si-based integratable micro-LIB systems.

3.2 Fabrication of 3D micro-LIBs with Si as the active material

Most of the 3D Si-based micro-LIB systems were all fabricated on the patterned Si wafer or 2D planar Si substrate. An efficient Li-ion barrier layer must be introduced to eliminate the electrochemical effect from the Si substrate and reduce the influence on the other integrated lab-on-chip micro/nano devices. However, there exists another kind of promising 3D micro-LIB system, in which the 3D-patterned Si substrate is expected to have dual effects as both the supporting structure and active anode material. The corresponding fabrication process can also be compatible with the current IC technologies. Moreover, when the 3D wafer-scale micro-LIBs were sliced into many independent units with a sound package, they also showed potential integratibility with the smart micro/nano-devices and displayed favorable properties in a wide range of practical applications [73–75].

As shown in Fig. 16(a) [76], Lethien et al. proposed the concept of a 3D all-solid-state Si/LiPON/$LiFePO_4$ micro-LIB. First, the 3D self-aligned and high-aspect-ratio silicon nanopillars (Si NPL) were obtained by the deep reactive ion etching (DRIE) and the photolithography processes (Figs. 16(b) and 16(c)). Then, the LiPON/$LiFePO_4$ (electrolyte/cathode) dual layers, as shown in Fig. 16(d), were consecutively and successfully deposited on the above 3D Si NPL surface by using the RF sputtering equipment. The fabrication process of this all-solid-state micro-LIB was performed by the Si-compatible technologies and would be beneficial for the integration with other micro/nano electronic devices. However, this micro-sized anode may present poor electrochemical performance due to the volume expansion during the cycling and intrinsic low electronic/ionic conductivities in the Si electrode [77,78]. Therefore, an alternative and effective strategy is required to circumvent the corresponding negative effects.

Recently, as shown in Fig. 17 [79,80], unique 3D nano-sized hexagonal Si nanorod (NR) arrays were successfully fabricated on the Si-wafer using the monolayer PS (Polystyrene) templates by the ICP dry etching technology. The monolayer PS nanosphere templates can be successfully prepared on the Si-wafer using the simple, low-cost, environmental-friendly, and self-assembled spin-coating method. Most importantly, the electrochemical Li storage ability of the 3D Si NR electrodes can be efficiently improved by fabricating 3D Si-based composite anodes using Si-compatible technologies to prepare different shells on Si [80–82].

By the radio frequency (RF)-magnetron sputtering

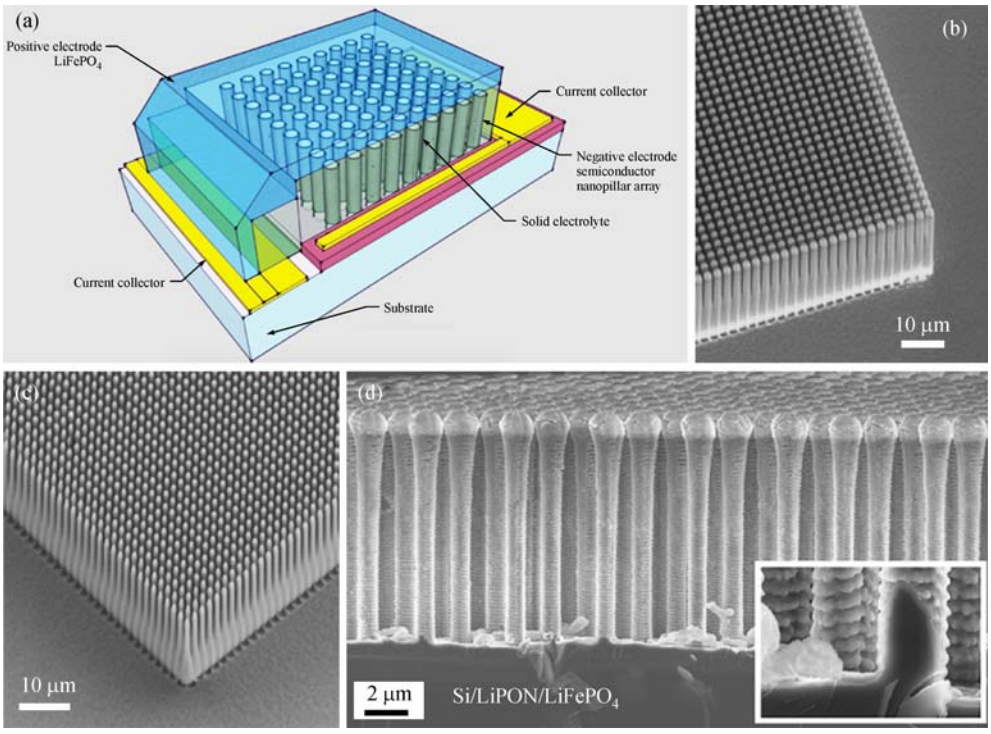

Fig. 16 (a) Overview of the 3D all-solid-state integrated micro-LIB; (b)–(d) SEM images of the Si NPL arrays after the LiPON/$LiFePO_4$ deposition. Reproduced with permission from Ref. [76], Copyright 2011, Elsevier

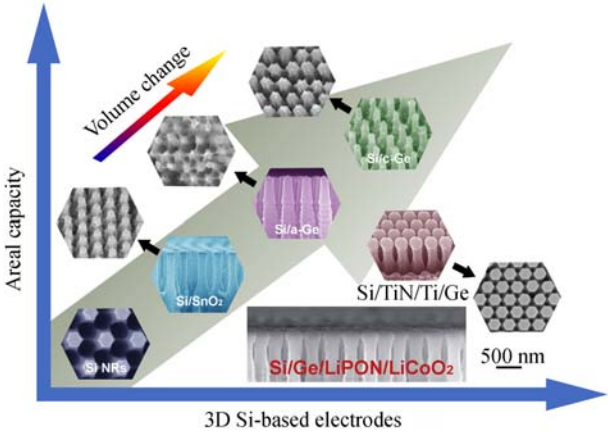

Fig. 17 Areal capacity vs. different 3D Si-based micro-LIB electrodes (black arrow: SEM images of the electrodes after Li-ion inserting/de-inserting process; bottom: SEM image of a 3D all-solid-state micro/nano-LIB arrays in the section view) [79–82]. Reproduced with permission from Ref. [83], Copyright 2016, American Chemical Society; Reproduced with permission from Ref. [84], Copyright 2015, Wiley-VCH

technique, amorphous or polycrystalline composite shells, e.g., Ge or SnO_2, can be deposited on 3D patterned Si NR arrays with improved electrode capacity [80,81]. Furthermore, compared with the amorphous Ge (a-Ge) shell electrode, the single-crystal Ge (c-Ge) composite electrode was also produced by the ultrahigh-vacuum chemical vapor deposition (UHV-CVD) process, which helped achieve even higher areal capacities in the corresponding electrode due to the improved electron/ion conductivities [82]. However, owing to the large volume expansion observed in the single-crystal Si core electrode, obvious capacity rising phenomenon and poor cycling performance can be observed in these kinds of composite electrodes. Therefore, the TiN/Ti interlayer concept was proposed, and the 3D multilayer Si/TiN/Ti/Ge NR composite electrode arrays were successfully prepared by the consecutive sputtering process [83]. The TiN/Ti interlayer has dual effects: 1) As the effective current collector that improves the electronic conductivity of the whole electrode, and 2) as the efficient Li-ion barrier layer preventing more Li ions from continuously inserting into the 3D Si substrate electrode. As a result, the improved energy storage properties and cycling stability in the 3D Si patterned composite electrode can be accomplished.

Additionally, the 3D Si/TiN/Ti/Ge NR composite electrode arrays also exhibited excellent cycling stability and rate capability as anode material for micro-sodium ion batteries (micro-SIBs) [84]. Within the composite electrode, the 3D Si NR arrays acted as the battery supporting structure, whereas the Ge shell proved to be the only active material for sodium ion (Na^+) storage, and the TiN/Ti interlayer efficiently played a positive role in electron transportation. Furthermore, the 3D Si/Ge/LiPON/$LiCoO_2$ all-solid-state micro/nano-LIB arrays can be fabricated via the consecutive sputtering process. These works provide

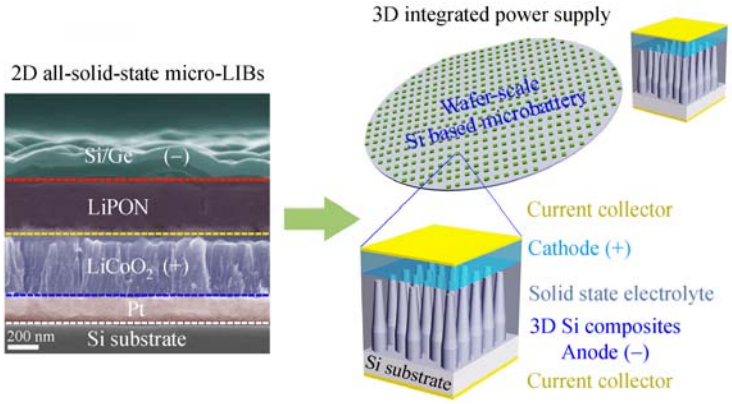

Fig. 18 Optimization of a Si-based all-solid-state micro-LIB from 2D to semi-3D

important experimental verifications for the development of the future 3D Si-based micro/nano-energy storage systems.

A variety of 3D Si-based NR composite electrode arrays were successfully fabricated, by using the semiconductor-compatible processing technologies with improved electrochemical energy storage performances during the half-cell testing. However, measuring the areal capacity of a full unit of the 3D all-solid-state micro/nano-LIBs remains a challenge due to the small thickness of the solid-state electrolyte and cathode electrode materials. Moreover, the short-circuit phenomena may also be another challenge for this micro/nanoscale-sized 3D Si-based all-solid-state LIBs. Therefore, in order to resolve the above issues, as shown in Fig. 18, a semi-3D micro/nano-LIB concept was then presented upon considering the merits of both the 3D micro/nano configuration and the 2D all-solid-state thin-film LIBs. The solid-state electrolyte was filled in the 3D Si-based NR composite electrodes; subsequently, the thin-film cathode and the corresponding current collector were finally deposited on the electrolyte surface. Thus, the areal capacity would be further improved due to the increased amount of Li-ion source from the solid-state electrolyte. Moreover, if the distance between the anode and the cathode could be enlarged, the short-circuit phenomenon may be eliminated. Hopefully, this semi-3D Si-based micro/nano-LIB system might present improved electrochemical performance with great potential application to power M/NEMS devices.

Compared with the current relatively mature anode preparation technology, the electrolyte and cathode materials are important factors that influence the electrochemical performance of a battery. For instance, the much lower ionic conductivity in solid-state electrolyte compared with the common liquid electrolyte is still an issue. Moreover, the conformal deposition of both electrolyte and cathode materials in different 3D Si-based microbattery structures is another formidable challenge. Therefore, the novel microbattery electrolyte and cathode material, along with their corresponding fabrication technologies, should be further investigated and improved.

4 Conclusions

In summary, micro/nano-energy storage systems, especially the micro-LIB system with compatible fabrication process with the IC chips, are popular research topics. Compared with the 2D thin-film LIBs, various 3D micro-LIBs have been successfully prepared to improve the battery storage capacity and rate capability in a limit footprint area. Among them, the 3D Si-based micro-LIB energy storage system is one of the best candidates due to the use of high-capacity Si anode, wafer-scale fabrication, and Si-compatible processing technologies.

In this review, 3D wafer-scale Si-based micro-LIBs and their corresponding fabrication approaches were presented. ALD, CVD and sputtering technique are the major methods used to deposit battery components on the 3D Si-based substrate. Fabricating semi-3D Si-based, all-solid-state micro-LIBs may be one of the promising ways to achieve further progress. However, many challenges should be overcome, such as the requirement of higher quality film and shorter-period deposition technique, battery structure optimization, higher ionic conductivity solid-state electrolyte fabrication, and so on. Therefore, more efforts should be exerted in this scientific field towards practical applications in autonomous micro/nano-smart devices.

Acknowledgements This work was financially supported by the National Basic Research Program of China (Grant No. 2015CB932301), the National Natural Science Foundation of China (Grant Nos. 61675173 and 61505172), the Natural Science Foundation of Fujian Province of China (Grant No. 2017H6022), and by the Science and Technology Program of Xiamen City of China (Grant Nos. 3502Z20161223 and 3502Z20144079).

References

1. WHAT IS A TRANSISTOR? Retrieved from http://www.kidbots.com/howto/HOW_TO_4.html
2. Intel Core i7-5960X, -5930K And-5820K CPU Review: Haswell-E Rises. Retrieved from http://www.tomshardware.com/reviews/intel-core-i7-5960x-haswell-e-cpu,3918.html
3. IBM's crazy-thin 7 nm chip will hold 20 billion transistors. Retrieved from http://www.pcworld.com/article/2946124/ibm-reveals-worlds-first-working-7nm-processor.html
4. Growing in maturity, the MEMS industry is getting its second wind. Retrieved from http://electroiq.com/blog/2015/05/growing-in-maturity-the-mems-industry-is-getting-its-second-wind/
5. Hu Y S, Demir-Cakan R, Titirici M M, et al. Superior storage performance of a Si@SiO_x/C nanocomposite as anode material for lithium-ion batteries. Angewandte Chemie International Edition, 2008, 47(9): 1645–1649
6. Xin X, Zhou X, Wang F, et al. A 3D porous architecture of Si/graphene nanocomposite as high-performance anode materials for Li-ion batteries. Journal of Materials Chemistry, 2012, 22(16): 7724–7730
7. Wang C, Taherabadi L, Jia G, et al. C-MEMS for the manufacture of 3D microbatteries. Electrochemical and Solid-State Letters, 2004, 7 (11): A435–A438
8. Talin A A, Ruzmetov D, Kolmakov A, et al. Fabrication, testing, and simulation of all-solid-state three-dimensional Li-ion batteries. ACS Applied Materials & Interfaces, 2016, 8(47): 32385–32391
9. West W C, Whitacre J F, White V, et al. Fabrication and testing of all solid-state microscale lithium batteries for microspacecraft applications. Journal of Micromechanics and Microengineering, 2001, 12 (1): 58–62
10. O'regan B, Grätzel M. A low-cost, high-efficiency solar cell based on dye-sensitized colloidal TiO_2 films. Nature, 1991, 353(6346): 737–740
11. Lee S K, Son S H, Kim K S, et al. Development of nuclear microbattery with solid tritium source. Applied Radiation and Isotopes, 2009, 67(7–8): 1234–1238
12. Sprague I B, Dutta P. Performance improvement of micro-fuel cell by manipulating the charged diffuse layer. Applied Physics Letters, 2012, 101(11): 113903
13. Yang Y, Pradel K C, Jing Q, et al. Thermoelectric nanogenerators based on single Sb-doped ZnO micro/nanobelts. ACS Nano, 2012, 6 (8): 6984–6989
14. Tarascon J M, Armand M. Issues and challenges facing rechargeable lithium batteries. Nature, 2001, 414(6861): 359–367
15. Sodium as alternative to lithium in batteries. Retrieved from http://neutronsources.org/news/scientific-highlights/towards-sodium-ion-batteries-understanding-sodium-dynamics-on-a-microscopic-level.html
16. How cells work. Retrieved from http://www.jmbatterysystems.com/technology/cells/how-cells-work
17. Zero electric motorcycles prove quiet, efficient, and fun. Retrieved from http://www.consumerreports.org/cro/news/2014/06/zero-motorcycles-electric-motorcycle-review/index.htm
18. Infinite Power Solutions, Inc. Retrieved from http://www.cytech.com/products-ips
19. Powering New Product Innovation. Retrieved from http://www.cymbet.com/
20. 11- and 13-inch MacBook Air (Late 2010). Retrieved from http://www.macworld.com/article/1155186/macbook_air.html
21. Panel G M. Transportation in the 21st Century. Retrieved from http://evworld.com/article.cfm?storyid = 1529
22. Stop going over your data-ways to preserve your cell phone data. Retrieved from https://www.puretalkusa.com/blog/preserve-your-cell-phone-data/
23. Hospital trust implants world's first MRI-safe pacemaker. Retrieved from http://www.westhertshospitals.nhs.uk/newsandmedia/mediar-eleases/2012/august/mri_safe_pacemaker.asp
24. Technology boosts Zambian health and outbreak early warning systems. Retrieved from http://www.htxt.co.za/2013/07/24/technology-boosts-zambian-health-and-outbreak-early-warning-systems/1
25. Tiny swarming robots coming soon to eat your data. Retrieved from http://gajitz.com/tiny-swarming-robots-coming-soon-to-eat-your-data/
26. The ingestible electronic drug-delivery system. Retrieved from http://www.fastcompany.com/1150215/gadgets-you-can-swallow
27. Explore ink technology, technology engadget, and more! Retrieved from https://www.pinterest.com/pin/98868154290733762/
28. Dragonfly surveillance cyborg could aid pollination. Retrieved from http://www.eetimes.com/document.asp?doc_id = 1331215
29. Bates J B, Dudney N J, Neudecker B, et al. Thin-film lithium and lithium-ion batteries. Solid State Ionics, 2000, 135(1–4): 33–45
30. 3D batteries. Retrieved from http://www.southampton.ac.uk/~ssegroup/research/3dbatteries.shtml
31. Wang C, Taherabadi L, Jia G, et al. C-MEMS for the manufacture of 3D microbatteries. Electrochemical and Solid-State Letters, 2004, 7 (11): A435–A438
32. Wang W, Tian M, Abdulagatov A, et al. Three-dimensional Ni/TiO_2 nanowire network for high areal capacity lithium ion microbattery applications. Nano Letters, 2012, 12(2): 655–660
33. Cheah S K, Perre E, Rooth M, et al. Self-supported three-dimensional nanoelectrodes for microbattery applications. Nano Letters, 2009, 9(9): 3230–3233
34. Sun K, Wei T S, Ahn B Y, et al. 3D Printing of interdigitated Li-ion microbattery architectures. Advanced Materials, 2013, 25(33): 4539–4543
35. Kotobuki M, Suzuki Y, Munakata H, et al. Fabrication of three-dimensional battery using ceramic electrolyte with honeycomb structure by sol-gel process. Journal of the Electrochemical Society, 2010, 157(4): A493–A498
36. Notten P H L, Roozeboom F, Niessen R A H, et al. 3-D integrated all-solid-state rechargeable batteries. Advanced Materials, 2007, 19 (24): 4564–4567
37. Wang J, Du N, Zhang H, et al. Cu-$Si_{1-x}Ge_x$ core-shell nanowire arrays as three-dimensional electrodes for high-rate capability lithium-ion batteries. Journal of Power Sources, 2012, 208: 434–439
38. Bi Z, Paranthaman M P, Menchhofer P A, et al. Self-organized amorphous TiO_2 nanotube arrays on porous Ti foam for recharge-

able lithium and sodium ion batteries. Journal of Power Sources, 2013, 222: 461–466
39. Reddy A L M, Shaijumon M M, Gowda S R, et al. Coaxial MnO_2/carbon nanotube array electrodes for high-performance lithium batteries. Nano Letters, 2009, 9(3): 1002–1006
40. Wu H, Cui Y. Designing nanostructured Si anodes for high energy lithium ion batteries. Nano Today, 2012, 7(5): 414–429
41. Chan C K, Zhang X F, Cui Y. High capacity Li ion battery anodes using Ge nanowires. Nano Letters, 2008, 8(1): 307–309
42. Ortiz G F, Hanzu I, Lavela P, et al. Nanoarchitectured TiO_2/SnO: A future negative electrode for high power density Li-ion microbatteries? Chemistry of Materials, 2010, 22(5): 1926–1932
43. Li X, Cheng F, Guo B, et al. Template-synthesized $LiCoO_2$, $LiMn_2O_4$, and $LiNi_{0.8}Co_{0.2}O_2$ nanotubes as the cathode materials of lithium ion batteries. Journal of Physical Chemistry B, 2005, 109 (29): 14017–14024
44. Landi B J, Ganter M J, Cress C D, et al. Carbon nanotubes for lithium ion batteries. Energy & Environmental Science, 2009, 2(6): 638–654
45. Zoom into a computer chip. Retrieved from https://www.extremetech.com/extreme/191996-zoom-into-a-computer-chip-watch-this-video-to-fully-appreciate-just-how-magical-modern-microchips-are
46. Micronas sells more Hall sensors, earns less. Retrieved from http://www.electronics-eetimes.com/news/micronas-sells-more-hall-sensors-earns-less
47. La memoria DRAM impulsa el mercado de semiconductores, pero no por mucho tiempo. Retrieved from http://www.silicon.es/la-memoria-dram-impulsa-el-mercado-de-semiconductores-pero-no-por-mucho-tiempo-79577
48. Chan C K, Peng H, Liu G, et al. High-performance lithium battery anodes using silicon nanowires. Nature Nanotechnology, 2008, 3 (1): 31–35
49. Wu H, Chan G, Choi J W, et al. Stable cycling of double-walled silicon nanotube battery anodes through solid-electrolyte interphase control. Nature Nanotechnology, 2012, 7(5): 310–315
50. Yao Y, McDowell M T, Ryu I, et al. Interconnected silicon hollow nanospheres for lithium-ion battery anodes with long cycle life. Nano Letters, 2011, 11(7): 2949–2954
51. Chan C K, Patel R N, O'connell M J, et al. Solution-grown silicon nanowires for lithium-ion battery anodes. ACS Nano, 2010, 4(3): 1443–1450
52. Liu N, Wu H, McDowell M T, et al. A yolk-shell design for stabilized and scalable Li-ion battery alloy anodes. Nano Letters, 2012, 12(6): 3315–3321
53. Song T, Cheng H, Choi H, et al. Si/Ge double-layered nanotube array as a lithium ion battery anode. ACS Nano, 2012, 6(1): 303–309
54. Hertzberg B, Alexeev A, Yushin G. Deformations in Si-Li anodes upon electrochemical alloying in nano-confined space. Journal of the American Chemical Society, 2010, 132(25): 8548–8549
55. Chang J, Huang X, Zhou G, et al. Multilayered Si nanoparticle/reduced graphene oxide hybrid as a high-performance lithium-ion battery anode. Advanced Materials, 2014, 26(5): 758–764
56. Zhang W, Hu J, Guo Y, et al. Tin-nanoparticles encapsulated in elastic hollow carbon spheres for high-performance anode material in lithium-ion batteries. Advanced Materials, 2008, 20(6): 1160–1165
57. Nicolet M A. Diffusion barriers in thin films. Thin Solid Films, 1978, 52(3): 415–443
58. Etacheri V, Haik O, Goffer Y, et al. Effect of fluoroethylene carbonate (FEC) on the performance and surface chemistry of Si-nanowire Li-ion battery anodes. Langmuir, 2012, 28(1): 965–976
59. Jung S C, Han Y K. How do Li atoms pass through the Al_2O_3 coating layer during lithiation in Li-ion batteries? Journal of Physical Chemistry Letters, 2013, 4(16): 2681–2685
60. Baggetto L, Knoops H C M, Niessen R A H, et al. 3D negative electrode stacks for integrated all-solid-state lithium-ion microbatteries. Journal of Materials Chemistry, 2010, 20(18): 3703–3708
61. Baggetto L, Niessen R A H, Roozeboom F, et al. High energy density all-solid-state batteries: A challenging concept towards 3D integration. Advanced Functional Materials, 2008, 18(7): 1057–1066
62. Oudenhoven J F M, Baggetto L, Notten P H L. All-solid-state lithium-ion microbatteries: A review of various three-dimensional concepts. Advanced Energy Materials, 2011, 1(1): 10–33
63. Xie J, Oudenhoven J F M, Li D, et al. High power and high capacity 3D-structured TiO_2 electrodes for lithium-ion microbatteries. Journal of the Electrochemical Society, 2016, 163(10): A2385–A2389
64. Eustache E, Tilmant P, Morgenroth L, et al. Silicon-microtube scaffold decorated with anatase TiO_2 as a negative electrode for a 3D litium-ion microbattery. Advanced Energy Materials, 2014, 4(8): 1301612
65. Létiche M, Eustache E, Freixas J, et al. Atomic layer deposition of functional layers for on chip 3D Li-ion all solid state microbattery. Advanced Energy Materials, 2016, 7(3): 1601402
66. Gerasopoulos K, Pomerantseva E, McCarthy M, et al. Hierarchical three-dimensional microbattery electrodes combining bottom-up self-assembly and top-down micromachining. ACS Nano, 2012, 6 (7): 6422–6432
67. Orendorff C J, Doughty D. Lithium ion battery safety. Interface-Electrochemical Society, 2012, 21(2): 35
68. Zhang S S. A review on the separators of liquid electrolyte Li-ion batteries. Journal of Power Sources, 2007, 164(1): 351–364
69. Golodnitsky D, Yufit V, Nathan M, et al. Advanced materials for the 3D microbattery. Journal of Power Sources, 2006, 153(2): 281–287
70. Golodnitsky D, Nathan M, Yufit V, et al. Progress in three-dimensional (3D) Li-ion microbatteries. Solid State Ionics, 2006, 177(26): 2811–2819
71. Nathan M, Golodnitsky D, Yufit V, et al. Three-dimensional thin-film Li-ion microbatteries for autonomous MEMS. Journal of Microelectromechanical Systems, 2005, 14(5): 879–885
72. Min H S, Park B Y, Taherabadi L, et al. Fabrication and properties of a carbon/polypyrrole three-dimensional microbattery. Journal of Power Sources, 2008, 178(2): 795–800
73. Peng K, Jie J, Zhang W, et al. Silicon nanowires for rechargeable lithium-ion battery anodes. Applied Physics Letters, 2008, 93(3): 033105
74. Wan J, Kaplan A F, Zheng J, et al. Two dimensional silicon nanowalls for lithium ion batteries. Journal of Materials Chemistry A: Materials for Energy and Sustainability, 2014, 2(17): 6051–6057

75. Ge M, Fang X, Rong J, et al. Review of porous silicon preparation and its application for lithium-ion battery anodes. Nanotechnology, 2013, 24(42): 422001
76. Lethien C, Zegaoui M, Roussel P, et al. Micro-patterning of LiPON and lithium iron phosphate material deposited onto silicon nanopillars array for lithium ion solid state 3D micro-battery. Microelectronic Engineering, 2011, 88(10): 3172–3177
77. Thompson S E, Parthasarathy S. Moore's law: The future of Si microelectronics. Materials Today, 2006, 9(6): 20–25
78. Tauc J. Optical properties and electronic structure of amorphous Ge and Si. Materials Research Bulletin, 1968, 3(1): 37–46
79. Yue C, Li J, Kang J. Fabrication of the hexagonal Si nanorod arrays using the template of polystyrene nanospheres in monolayer dispersion. Proceedings of the Institution of Mechanical Engineers, Part N: Journal of Nanomaterials, Nanoengineering and Nanosystems, 2014, 228(1): 40–45
80. Yue C, Yu Y, Yin J, et al. Fabrication of 3D hexagonal bottle-like Si-SnO_2 core-shell nanorod arrays as anode material in on chip micro-lithium-ion-batteries. Journal of Materials Chemistry A: Materials for Energy and Sustainability, 2013, 1(27): 7896–7904
81. Li J, Yue C, Yu Y, et al. Si/Ge core-shell nanoarrays as the anode material for 3D lithium ion batteries. Journal of Materials Chemistry A: Materials for Energy and Sustainability, 2013, 1(45): 14344–14349
82. Yue C, Yu Y, Wu Z, et al. Enhanced reversible lithium storage in germanium nano-island coated 3D hexagonal bottle-like Si nanorod arrays. Nanoscale, 2014, 6(3): 1817–1822
83. Yue C, Yu Y, Wu Z, et al. High stability induced by the TiN/Ti interlayer in three-dimensional Si/Ge nanorod arrays as anode in micro lithium ion battery. ACS Applied Materials & Interfaces, 2016, 8(12): 7806–7810
84. Yue C, Yu Y, Sun S, et al. High performance 3D Si/Ge nanorods array anode buffered by TiN/Ti interlayer for sodium-ion batteries. Advanced Functional Materials, 2015, 25(9): 1386–1392